Urban Energy System Simulation using the Functional Mock-up Interface

Markus Schumacher, Marcus Fuchs, Dirk Müller
RWTH Aachen University, E.ON Energy Research Center,
Institute for Energy Efficient Buildings and Indoor Climate

Abstract

The growing level of complexity in urban energy systems (UES) makes integrated simulation models indispensable. Efforts to link models of different domains have been made, but only few integrated approaches exist. Most building simulation models show either high computational effort or a low level of detail, which reduces their applicability for district analyses. The presented approach consistently uses reduced order models that only capture key effects for the simulation of UES, leading to comparably low computational effort. We make extensive use of open-source tools and show how the integration of those can be accomplished within a Python framework using the functional mock-up interface (FMI) standard. In order to adapt the environment to the purpose of a particular UES analysis, its individual modules are replaceable. Harnessing this flexibility, a case study was conducted, analyzing an UES of eight buildings with different structural and operational designs. In addition to the general feasibility of the proposed framework for simulation-based design of UES, the results show the positive effect of grid-driven electric heating devices (EHD) on the power grid. By this means, a reduction of the transformer flow bandwidth by 40 % is achieved.

Nomenclature

LB	Lower residual load bound for release/-forced operation
n	Number of released HP/CHP
$P_{\mathrm{App}}(t)$	Load of household appliances at time t
$P_{\mathrm{BES}}(t)$	Aggregated power demand for heating at time t
P_{el}	Electric capacity of EHD
$P_{\mathrm{PV}}(t)$	Photovoltaic generation at time t
P_{TF}	Transformer flow at time t
$P_{\mathrm{TF}}{}^{*}(t)$	Preliminary transformer flow at time t
$\dot{Q}_{\mathrm{th}}$	Thermal capacity of EHD
$T_{\mathrm{on/off,s}}$	Threshold storage temperature of Two-Point-Controller depending on grid state 0...2
T	Storage temperature at top/bottom
UB	Upper residual load bound for release/-forced operation
v_{m}	Voltage magnitude
x_{Mod}	Modulation range of EHD
BES	Building energy system
CHP	Combined heat and power
DHW	Domenstic hot water
DSM	Demand side management
EHD	Electric heating device
FMI	Functional mock-up interface
FMU	Functional mock-up unit
HP	Heat pump
MES	Multi energy systems
PV	Photovoltaic
TES	Thermal energy storage
UES	Urban energy systems

Introduction

The large deployment of renewable energy sources into the electrical grid will result in higher fluctuations and temporal overproduction of electricity. These fluctuations have to be continuously balanced by the grid operator. Since most residential buildings in Northern Europe still have a significant heat demand, building energy systems (BES), that are connected to the power grid, could be an option to mitigate these fluctuations. According to Arteconi et al. (2013) and Hedegaard and Münster (2013) demand side management (DSM) measures using EHDs, like heat pumps (HP) and combined heat and power

(CHP) units, are a promising approach in this context. In Müller et al. (2015) a broad review of EHD-based DSM concepts is conducted, also considering the restrictions that are imposed by building residents.

However, the quantification and demonstration of the balancing potential is a complex task, since suitable field tests would require the participation of a large amount of buildings, each equipped with grid coupled EHDs and grid responsive control systems. Therefore, multi-domain simulation models (especially electrical and thermal) should be considered. Furthermore, the fast and dynamic character of power systems calls for dynamic models, meaning that static approaches, that only rely on energy balances and representative periods are not sufficient (Rohjans et al. (2014)).

Concerning the modeling of the thermal domain, high-order dynamic simulation models are already of great importance in the building sector, with many different approaches applied (Modelica, TRNSYS, EnergyPlus etc.). These come with large computational effort and are therefore only suitable for the simulation of single buildings or small districts. Concerning the electrical grid domain, a variety of simulation tools exist with different focuses (Bam and Jewell (2005)). However, the aforementioned tools mostly consider only a single domain, which is insufficient for the analysis of multi energy systems (MES).

Integrated MES models of different character, are recently attaining importance (Mancarella (2013)). For this purpose, co-simulation seems to be a promising approach. Co-simulation models are able to bring together multiple domains, like electrical and thermal, as shown in Molitor et al. (2014) and Patteeuw et al. (2015). The combination of electric and communications domain, as in Mets et al. (2014), is also important for the evaluation of future smart grids. A classification of different co-simulation approaches was conducted in Schloegl et al. (2015).

Besides the aforementioned dynamics that are introduced by the electrical domain, novel approaches for UES modeling should explicitly be able to consider temperatures in hydronic circuits and not only energy balances. Based on this, an exergetic analysis of an UES is possible and temperature-dependent phenomena, like EHDs' efficiencies, can be represented. Furthermore, thermal energy storages (TES)are commonly seen as a key element to utilize the energy flexibility that buildings can offer (Arteconi et al. (2012), Stinner et al. (2016)). The capacity of water-based TES however changes significantly depending on their current temperature distribution. To cover these temperature-dependent effects, a dynamic physics-based approach that utilizes the capabilities of the modeling language Modelica, accompanied by the FMI standard (Blochwitz et al. (2012)) is proposed in our work.

The remainder of the paper is organized as follows. First, we describe the structure of the developed simulation environment. The utilized Modelica models and control strategies are presented in detail. On this basis, we introduce the case study which was conducted and analyze its simulation results. Using these results, we formulate some general conclusions.

Methods and Simulation

Structure of Simulation Environment

The aforementioned requirements to represent fast dynamics and temperature-dependent phenomena can be addressed by the usage of Modelica to represent the BES and PYPOWER for the simulation of electrical distribution grids (Lehnhoff et al. (2015)). The integration of both domains is done in Python. We use two packages called PyCity and uesgraphs. PyCity is used for data handling and scenario generation of city districts while uesgraphs defines a framework to represent buildings and energy networks in a geo-referenced system graph. Open-source releases of both packages are planned for the future. In combination, these tools provide an object-oriented structure for modeling of UES. With this environment, multiple building entities can be created, each of which holds several specific attributes including:

- Geographical position
- Type of heat supply system
- Type of domestic hot water (DHW) production
- Stochastic occupancy profile (based on Richardson et al. (2008))
- Stochastic DHW demand profile (based on Beausoleil-Morrison and Arndt (2008))
- Electric loads
  - Photovoltaic (PV) production
  - Appliances load (based on Richardson et al. (2010))
  - Power demand for DHW preparation
- Description of Modelica BES model as functional mock-up unit (FMU)

Making use of the above attributes the FMU can be simulated for each time step in a given period, leading to a residual electric load and space heating demand profile.

Together, the individual building entities form an UES, that can be geographically described, using the position attribute of each entity. Based on this, a network-graph, implemented in uesgraphs, can be created. Figure 1 shows the structure of the simulation environment.

Following this approach, the space heating demand is calculated via a Modelica model, wrapped into an FMU. The FMU integration into the PyCity platform was done with the open-source PyFMI package (Bastian et al. (2011), Andersson (2016), Andersson et al. (2016)).

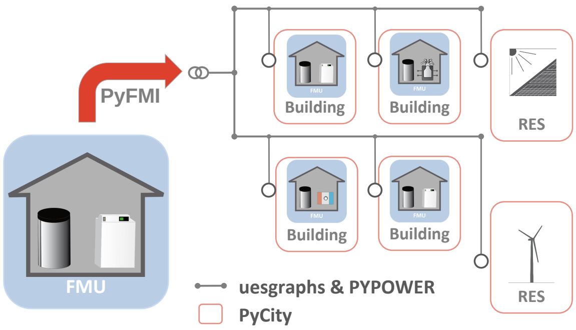

Figure 1: Schematic of integral simulation environment

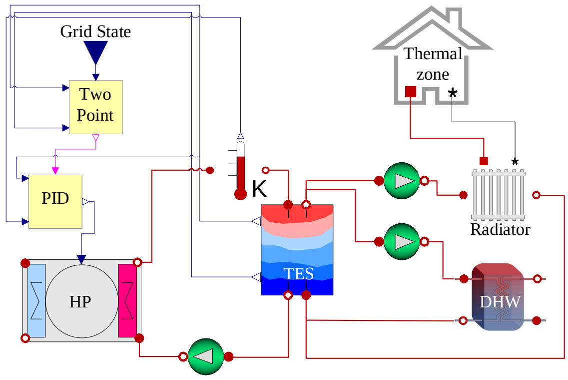

Figure 2: Schematic of BES with EHD

Building Energy System Model

The structure of an exemplary Modelica BES model, that is wrapped into an FMU, is shown for an HP system in figure 2.
Each FMU contains a dynamic low-order building model (Lauster et al. (2014)), representing a single zone building, which is implemented using the open-source Modelica library AixLib[1] (Müller et al. (2016)). The parameterization of this model was done with TEASER[2], a Python tool for automated generation of building models (Remmen et al. (2016)).
In addition to the building model, the FMU also contains the entire hydronic system, including the EHDs and the emission system. These parts of the model are implemented using the Modelica library FastHVAC by Stinner et al. (2015).
In addition to the EHDs, also a stratified TES is part of the BES, to enable the utilization of the building's potential energy flexibility. The heat emission is modeled with a radiator model, including a thermostatic valve, that is connected to the thermal zone model. The desired temperature of the thermal zone is set to 20 °C throughout the year, with no night-setback considered. Furthermore, a multi-layer heat exchanger model serves as DHW station. For DHW preparation, fluid is drawn from the top level of the TES and fed to the heat exchanger, heating fresh water from 10 °C to 45 °C. The controls of the BES are integrated into the Modelica model as well and will be explained in the next section.
The state of the described BES model depends on several outer influences, that are considered as model inputs. The main inputs are weather data, providing the outdoor temperature as well as relevant radiation data. Furthermore, the DHW mass flow profile and the electrical grid status are fed into the model. The latter carries information for the EHD controller which of the implemented control strategies is activated.
Since the simulation environment follows a closed-loop approach, the BES itself also influences the state of the UES by injection or consumption of electric energy. Therefore, each BES, and thus also FMU, is linked back to the surrounding system layer.

Control Strategy

General topology

The control logic of the UES is divided into a district level, represented by an aggregation module, and a building level. On the district level, an aggregation algorithm determines the current demand for flexibility based on the grid status at a given time step. Additionally, the aggregation algorithm gathers information about the current flexibility potential from the individual BES and in turn tries to match supply and demand. The flexibility demand can be either positive, which would require an increased electricity generation by CHP devices, or negative, which would in turn call for additional loads, such as electric HPs. The result of the matching problem is an operational release plan, that is passed to the individual building level controls. To be able to achieve particular goals for the UES, e.g. reduction of transformer flows or control of voltage magnitudes, the aggregation module is designed to be replaceable. With this feature, different controls can be tested and evaluated.

Grid Level

To investigate the impact that different control concepts have on the grid status, the following aggregation algorithms were considered in this paper:

- Heat-driven
- Uniform aggregation
- Coordinated aggregation

In the heat-driven control concept the EHDs have no information about the grid status and operate purely heat-driven. This control concept will serve as a reference since it is state of the art. The second concept uses the current transformer flow as grid status, where positive values indicate that the current power demand of the distribution grid exceeds the local production. In that case, all CHPs are released, meaning the individual devices make use of storage capacity

[1] https://github.com/RWTH-EBC/AixLib
[2] https://github.com/RWTH-EBC/Teaser

which is provided by the TES. This way, the heat generation can be systematically shifted in time. A negative transformer flow consequently releases the HP devices.
In contrast to that, the third concept controls the EHDs individually. To coordinate the operation of different EHD technologies, a desired and a maximum bandwidth for the transformer flow is implemented. The former is defined by the upper and lower bounds UB_{Release} and LB_{Release}. It represents a transformer flow range, where the grid devices' secure operation is assured. The latter bandwidth is determined by UB_{Force} and LB_{Force}. Leaving this transformer flow range puts the secure operation of the distribution grid at stake, and should therefore be avoided.
The flow structure of the coordinated aggregation algorithm is depicted for the HP case in figure 3 and will be explained in the following.
Based on the district's aggregated power demand for heating of the previous time step $P_{\mathrm{BES}}(t-1)$ and the non-heating related building loads, formed by the local PV generation $P_{\mathrm{PV}}(t)$ and the load for household appliances $P_{\mathrm{App}}(t)$, a preliminary transformer flow ${P_{\mathrm{TF}}}^*(t)$ is calculated[3]. Depending on the transformer flow's sign, one of the aggregator algorithm branches is activated. In both branches the initial schedule releases the operation for all devices, i.e. HPs and CHPs. In the following, we will describe the algorithm for the case of a positive transformer flow.
After activation of the positive branch, the algorithm first checks whether the transformer flow is below the upper bound UB_{Release}. If this condition holds, the aggregation is finished and all EHDs have an operational release for the current time step. Based on this, the FMUs of the entire UES are simulated. The simulation's result is a final value for $P_{\mathrm{BES}}(t)$.
If the transformer flow is above UB_{Release}, the algorithm checks if the number of released HPs is above zero. In that case, one of the HPs is blocked in the current aggregation by withdrawing its operational release[4]. Based on the new planning, a preliminary value for the aggregated BES load ${P_{\mathrm{BES}}}^*(t)$ is calculated and the aggregation starts a new iteration. However, if the number of released HPs is already zero, the algorithm checks if also the upper bound UB_{Force} is violated. For this case, an available CHP is forced into operation.
Based on this release plan a new preliminary aggregated BES load is calculated and another iteration is initiated. The iteration stops as soon as the transformer flow is within the release bounds or the flexibility potential of all devices is depleted. The iterated plan is used to simulate the final aggregated BES load. A similar aggregation is performed for negative transformer flows by first blocking CHPs and then forcing HPs into operation.

[3]The PV generation is incorporated as a negative load
[4]The current implementation chooses the devices randomly

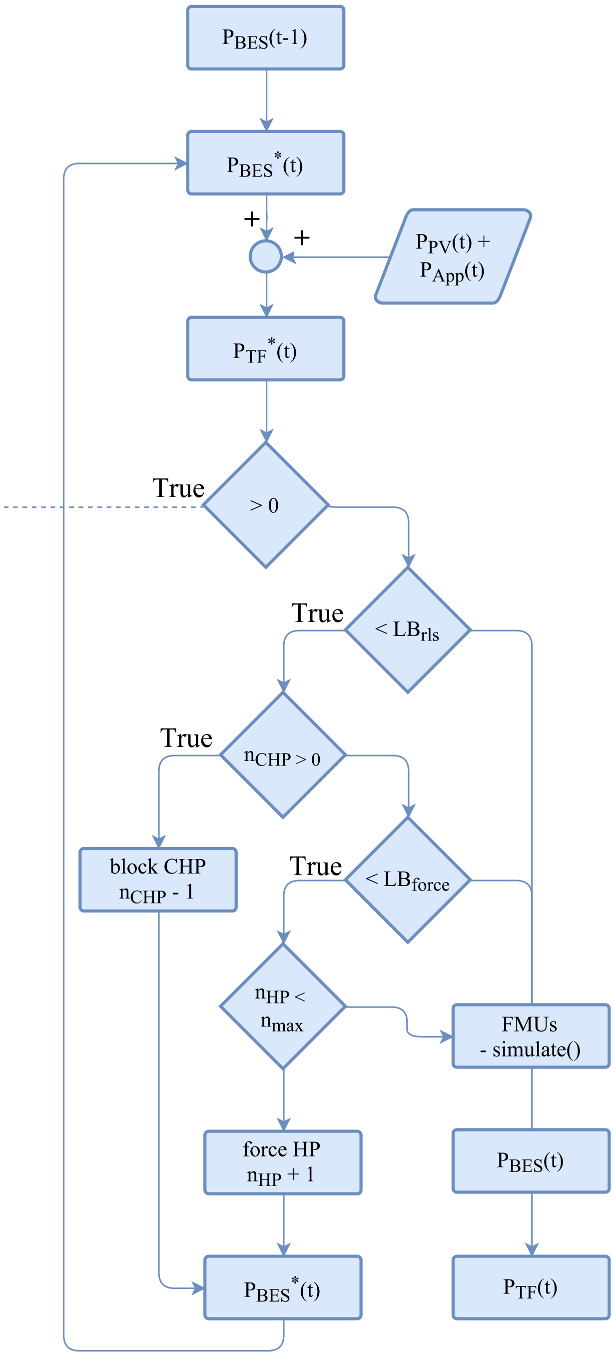

Figure 3: Grid level control strategy for HP case

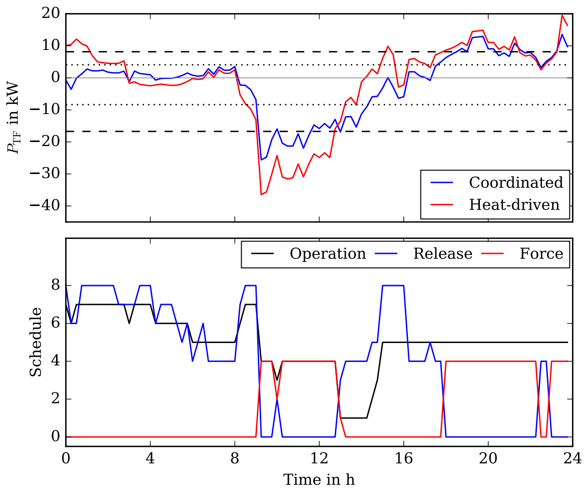

Figure 4: Scheduling example for single day

The result of the coordinated aggregation algorithm for one day in march is shown in figure 4. The dashed lines indicate the desired and forced bandwidth that are implemented in the grid level controller. In the first hours of the day all EHDs have a release, since the transformer flow is within the desired bandwidth. This way, HPs and CHPs can cooperate in supplying the districts heat demand.

However around 5 o'clock the resulting transformer flow would exceed its limits, causing the aggregation algorithm to block the HP operation. With an increasing solar irradiation, and consequently larger PV production in the morning hours, the transformer flow decreases, allowing the HPs to operate again. As the decrease continues, leading to an export of power to the higher level grid, the CHPs operation is blocked from now on. This leaves HPs as the only released devices.

Despite the CHP blocking, the transformer flow falls below its lower bound LB_{Force}. In that case, the forced operation of the HPs is activated for a short period of time, bringing back the transformer flow into its maximum allowable bandwidth. With lower PV production in the evening hours, the transformer flow increases again, which temporarily releases all EHDs. Finally the transformer flow gets positive again, which mainly leaves the CHPs in operation.

Building Level

The BES control is designed in a two level topology, with a two-point controller on the top level and a PID controller on the lower level (see figure 5). As long as the top level controller sends an internal release to the PID, which indicates that the TES temperature is below its maximum, the EHD is set to operate.

As mentioned before, each BES in the considered environment is able to operate in a grid-driven mode. To integrate this ability into the control concept, the operational release signal, coming from the grid level, is used to communicate the current grid state to an individual BES. This signal distinguishes three different grid states, which all have particular aims:

- State 0: No grid release granted. Minimize EHD operation, while fulfilling the building's heat demand
- State 1: Grid release granted. EHD can operate in heat-driven mode and charge the TES if necessary
- State 2: Forced EHD operation with maximum possible heat output until the TES is fully charged

Additionally, the current state of the TES influences whether a granted release actually leads to operation of a device. To integrate the necessary information about the TES, the temperatures T_{Top} and T_{Bottom} are fed to the two-point controller as well. By this means, both operational dependencies can be linked to each other. To prevent the EHD from fully charging the TES in case of high grid-stress (e.g. large transformer flows or high voltage deviations) the external release signal is also used to adapt the state-dependent threshold temperature of the controller hysteresis $T_{\text{on/off,s}}$. An internal release signal for the PID is granted, if the top storage temperature T_{Top} is below the current threshold temperature $T_{\text{on/off,s}}$. Accordingly, the EHD operation is stopped, as soon as the bottom TES temperature T_{Bottom} exceeds the threshold temperature $T_{\text{on/off,s}}$. The lowest acceptable threshold temperature in the considered concept is set to 45 °C, ensuring the heat supply of the building, while still reducing the grid interaction to a minimum. The maximum threshold is 60 °C for the HP and 80 °C for the CHP respectively.

The EHD's output can be modulated in the range x_{Mod} of 35 to 100 % of its nominal value for the HP and 25 to 100 % for the CHP respectively. It is finally controlled by the PID controller. The flow temperature of the EHD is set in such a way, that it is able to charge the top storage layer.

An exemplary EHD operation is depicted in figure 6, showing one day in the transition season.

Beginning with a grid release, the HP starts-up at full load until T_{Top} achieves the desired value of 55 °C, and in turn the output is modulated. As soon as T_{Bottom} reaches the current threshold $T_{\text{On/Off,1}}$ the HP operation is immediately stopped. Afterwards the BES controller switches to state 2, leading to a forced device start-up. At the end of the day the HP operation is blocked from the grid level controller which results in a discharging of the TES.

Case Study

For this paper we conducted a case study, analyzing an UES of eight well insulated single family houses (SFH). Although the UES simulation for up to 64 buildings is already possible with the presented framework, we limited the consideration in order to

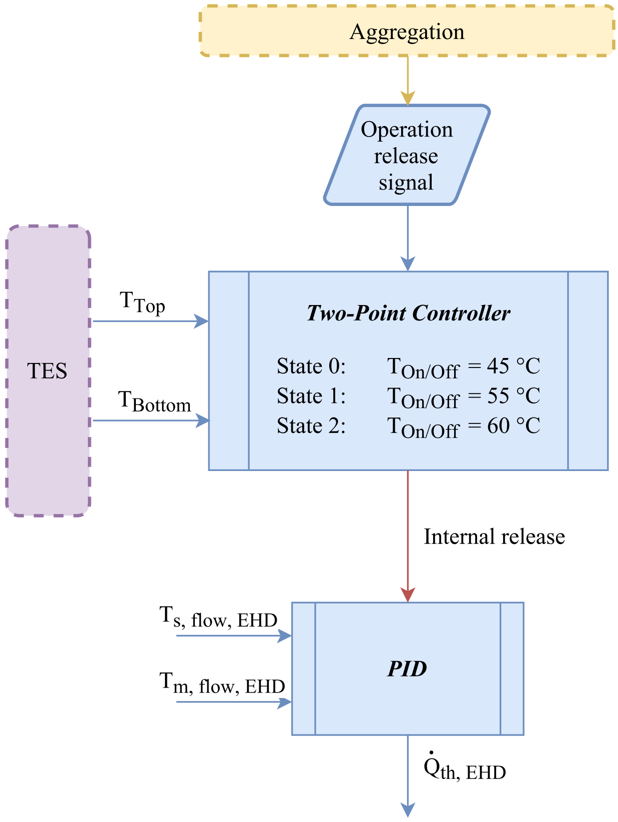

Figure 5: Control scheme of electric HP

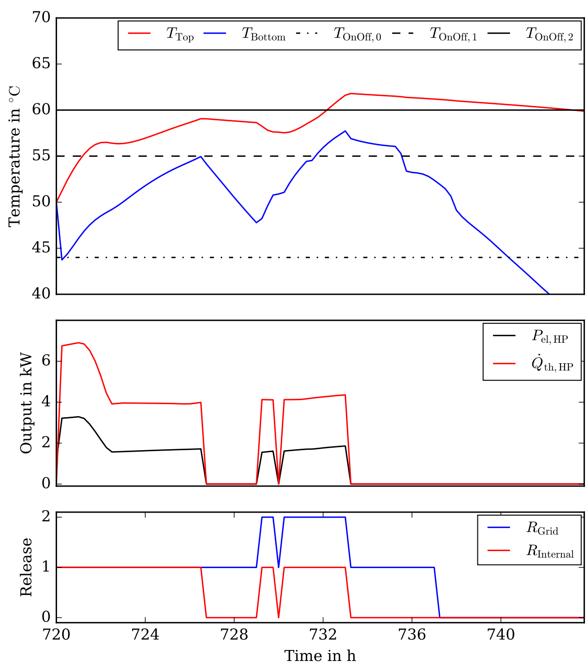

Figure 6: Exemplary operation of a HP

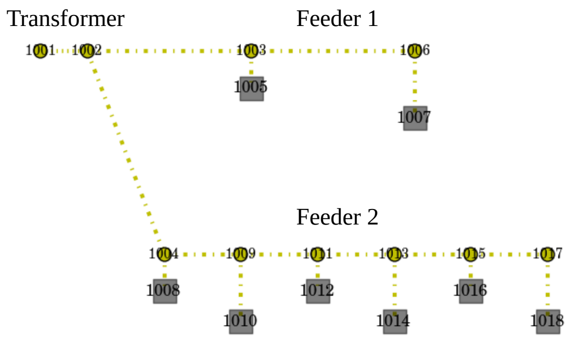

Figure 7: Network graph of considered distribution grid

demonstrate the general feasibility of the concept. The individual buildings have a living area of 240 m^2 and an annual space heat demand of 15.500 kWh per year. Each of them has 3 to 5 inhabitants and is equipped with a PV panel of 9 to 12 kW_p. To be able to analyze the impact of electrical loads as well as electricity generation on the distribution grid, four SFH comprise an HP, whereas the remaining four buildings use a CHP to supply the space heating and domestic hot water demand.

For the electrical domain we considered a rural, low voltage electrical grid, following the structure of a reference grid according to Kerber and Witzmann (2008). The reference grid consists of a MV/LV transformer and two grid feeders (see figure 7). Feeder 1 only comprises two buildings, one equipped with a CHP and the other with an HP. Feeder 2 is formed by the remaining buildings, that either comprise an HP or CHP and a PV panel. The grid connections are created via underground cables, resulting in two network nodes per building.

Furthermore, the case study considers the three aforementioned control concepts heat-driven, uniform and coordinated aggregation. For the coordinated aggregation we determined a desired and forced bandwidth of 25 % and 50 % of the maximum non-heating residual load, which is formed by the PV and appliances load.

Since one purpose of the presented simulation environment is to assess the impact of EHD technologies on the electrical grid operation, the model parameterization is of great importance. The set of main parameters that describe the BES in the considered case study is listed in table 1.

Table 1: Main EHD parameters

Parameter	HP	CHP
P_{el}	4 kW	4 kW
$\dot{Q}_{\mathrm{th}}$	10.8 kW	10.4 kW
x_{Mod}	35...100 %	25...100 %

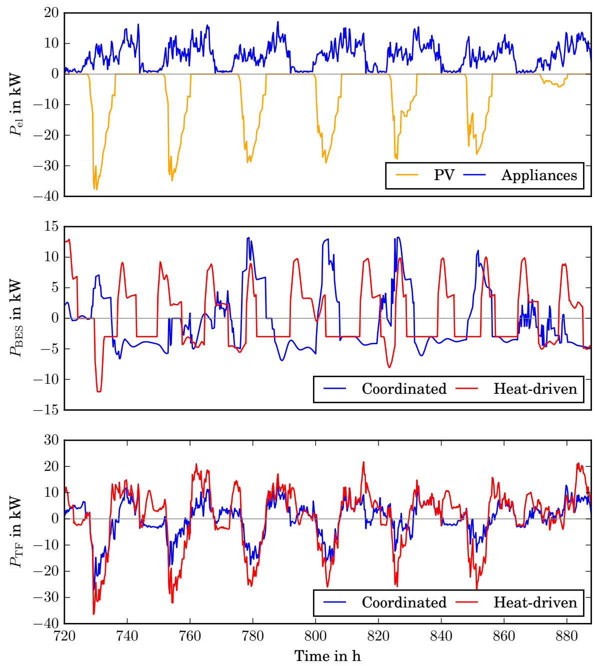

Figure 8: Components of the transformer flow

Results and Discussion

General

To assess the feasibility of the presented approach for simulation-based design of UES, we conducted simulations of several exemplary weeks. In the following we will focus on the first week of march (Monday to Sunday). Besides the general feasibility, we want to show the adaptability of the proposed framework. Therefore we analyze the results of two different aggregation algorithms in comparison to a reference and show their impact on the grid operation.

This evaluation of the grid impact of EHD is done with mainly two measures, the transformer flow P_{TF} and the voltage magnitude v_{m}. Firstly, they give precise information about how much electricity can be produced and consumed directly on the low voltage level. Secondly, they show if the operational constraints of the grid are not violated.

Moreover, we give a brief overview on computational questions that arise with the considered approach and how these can be addressed in future works on this matter.

Application

Figure 8 shows the individual components, that form the transformer flow. The upper plot shows the aggregated PV and appliances load. Together they form the non-heating related residual load of the district. The electrical load induced by the EHDs is added to this residual load and shown in the next plot for a heat-driven and balanced operation. Adding up the latter components results in the transformer flow of the considered distribution grid. It can be seen, that the aggregation algorithm is able to shift the EHD operation away from peak hours, which leads to a smoothed transformer flow.

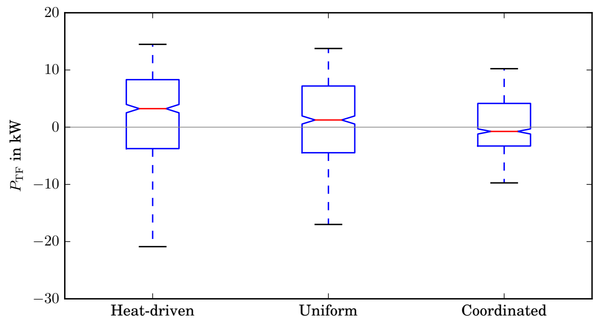

Figure 9: Transformer flow in heat-driven, uniform and coordinated aggregation mode

Harnessing the replaceability of individual components of the simulation environment, the influence of different aggregation algorithms can be assessed. Figure 9 shows the grid balancing potential of three different control schemes, that were considered in the underlying case study.

The standard heat-driven operation is determined as reference. Furthermore, a uniform EHD operation is possible, where positive transformer flows release all CHPs and negative ones release all HPs. It can be seen, that already the uniformly grid-driven control scheme is able to reduce the negative peak transformer flow. However, the positive peak can only be marginally reduced and the size of the box, that covers both inner quartiles, is hardly influenced. Switching from the uniformly to the coordinated grid control approach, that was introduced before, significant peak reductions on the positive and negative side can be found. Additionally the size of the box is reduced and the mean value of the transformer flow is close to zero.

Although the considered aggregation algorithms are able to improve the grid conditions, the presented results are non-optimal. Both strategies lack an optimal scheduling, that is based on a load forecast. In comparison to optimal approaches, as in Molitor et al. (2013) and Harb et al. (2015), the degree of coordination has to be further improved. This will be done by introducing an optimized scheduling procedure to the environment in upcoming developments. Also the integration of flexibility indicators (Stinner et al. (2016)) into the operation are likely to have a positive effect on the balancing performance.

Using the power flow calculation method of PY-

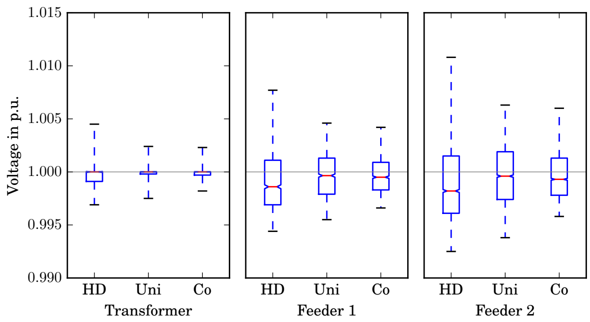

Figure 10: Voltage magnitude in grid feeders

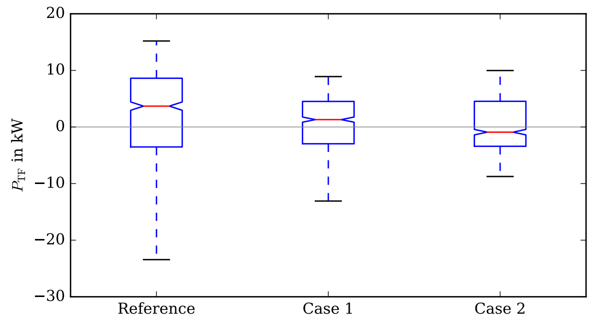

Figure 11: Influence of desired bandwidths on the transformer flow

POWER, the evaluation of voltage magnitudes within the grid is possible. For this purpose the voltage is referenced to the desired voltage of 220 V and therefore expressed in per unit (p.u.). Figure 10 shows the results of the power flow calculation in the aforementioned grid feeders for three different control strategies.

The heat-driven control strategy shows comparably high voltage deviations. Especially in feeder 3, where the majority of buildings is placed and therefore the PV injection is high, the voltage reaches a high level with significant peaks. The other feeder and the transformer show lower voltage deviations. However, in all feeders the change to a uniformly grid driven control scheme is already able to increase the voltage stability. Additionally, the mean values and the center of the voltage magnitude are moved closer to 1.0, which is the ideal value. Further improvements can be achieved by using the coordinated aggregation algorithm, that orchestrates the individual EHDs within the distribution grid.

Besides replaceability of entire modules, the presented environment facilitates parameter studies. For this purpose, we analyzed the impact, that a change in bandwidths of the coordinated aggregation algorithm has on the grid balancing. Figure 11 shows a comparison of two different algorithm setups to the heat-driven reference case. In case 1 the bandwidth remains at 25 and 50% of the maximum non-heating residual load as explained before. For the second case the bandwidth was reduced to 15 and 30 %.

As already mentioned before, a significant reduction of peak transformer flows is possible by introducing the coordinated aggregation method to the UES. If we further reduce the inner and outer bounds parameters, this leads to a even better reduction of negative peaks. However, there is no further improvement possible on positive peaks. In fact, the maximum positive transformer flow is slightly increased, which could not be expected upfront.

The reason for this result can be found in the non-optimal scheduling of the EHDs, where the devices' flexibility might be used up in phases of low flexibility demand, that precede a high demand.

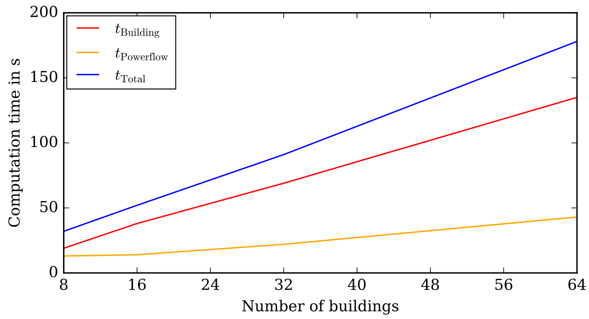

Figure 12: Computational effort depending on UES size

Computational Performance

Regarding practical applicability, the computational performance of the presented approach is an important issue. So far, both the simulation of the BES and power flow calculation of the distribution grid run in a single core framework. Nevertheless, it is already possible to run simulations on a larger scale. The timing results for the computational effort are depicted in figure 12.

It can be seen, that the simulation time for the BES scales nearly linear with the size of the district, which could be expected since the current approach manages the workload in a sequential way. However the power flow calculation generates an exponential workload with a growing number of building entities and their accompanying grid nodes. This effect can be a bottleneck in a future multi-core environment, since the good scalability of the BES simulations cannot be harnessed.

Conclusion

The presented environment clearly shows the feasibility of integrated UES simulation, using reduced order Modelica models wrapped into FMUs and PYPOWER. Following this approach, the interaction of buildings and the electrical grid can be computed in a dynamic and closed-loop manner.

The developed simulation environment is designed to be modular. By means of this, particular parts of the

environment can be replaced. Important design aspects of future UES, for instance different technology mixes and the correct dimensioning of BES, can be analyzed in a straight forward way. Furthermore, particular grid operation schemes can be implemented to assess their grid balancing potential.
By focusing on the key elements, that are important for large scale UES analysis, we can achieve good computational performance, while still preserving a high level of detail. Furthermore, the analysis shows that the simulation of medium scale UES with up to 64 buildings are possible even in a single core framework. Since the purpose of the presented environment is the simulation of large UES of several hundreds of buildings, the utilization of multiple processors is a prerequisite for future developments. Pursuing such an approach, for example by using multi-core PCs or PC clusters, is likely to significantly improve the computational performance and scalability towards large UES.

Acknowledgements

We gratefully acknowledge the financial support for this project by BMWi (German Federal Ministry of Economics and Energy) under promotional reference 03ET1390A. The project contributes to the IEA EBC Annex 67 "Energy Flexible Buildings".

References

Andersson, C. (2016). *Methods and Tools for Co-Simulation of Dynamic Systems with the Functional Mock-up Interface*. Ph. D. thesis, Lund University, Lund.

Andersson, C., J. Åkesson, and C. Führer (2016). *PyFMI: A Python Package for Simulation of Coupled Dynamic Models with the Functional Mock-up Interface*. Technical Report in Mathematical Sciences, Lund University, Lund.

Arteconi, A., N. J. Hewitt, and F. Polonara (2012). State of the art of thermal storage for demand-side management. *Applied Energy 93*, 371–389.

Arteconi, A., N. J. Hewitt, and F. Polonara (2013). Domestic demand-side management (DSM): Role of heat pumps and thermal energy storage (TES) systems. *Applied Thermal Engineering 51*(1-2), 155–165.

Bam, L. and W. Jewell (2005). Review: power system analysis software tools. In *IEEE Power Engineering Society General Meeting, 2005*, pp. 146–151.

Bastian, J., C. Clauß, S. Wolf, and P. Schneider (2011). Master for Co-Simulation Using FMI. In C. Clauß (Ed.), *Proceedings of the 8th International Modelica Conference, March 20th-22nd, Technical Univeristy, Dresden, Germany*, Volume 63 of *Linköping electronic conference proceedings*, pp. 115–120. Linköping: Univ. Electronic Press.

Beausoleil-Morrison, I. and U. Arndt (2008). *An experimental and simulation-based investigation of the performance of small-scale fuel cell and combustion-based cogeneration devices serving residential buildings: Final report of Annex 42 of the International Energy Agency's Energy Conservation in Buildings and Community Systems Programme.* Ottawa: Natural Resources Canada.

Blochwitz, T., M. Otter, J. Akesson, M. Arnold, C. Clauß, H. Elmqvist, M. Friedrich, A. Junghanns, J. Mauss, D. Neumerkel, H. Olsson, and A. Viel (2012). Functional Mockup Interface 2.0: The Standard for Tool independent Exchange of Simulation Models. In M. Otter and D. Zimmer (Eds.), *Proceedings of the 9th International Modelica Conference*, pp. 173–184. Linköping: Modelica Association.

Harb, H., J.-N. Paprott, P. Matthes, T. Schütz, R. Streblow, and D. Müller (2015). Decentralized scheduling strategy of heating systems for balancing the residual load. *Building and Environment 86*, 132–140.

Hedegaard, K. and M. Münster (2013). Influence of individual heat pumps on wind power integration – Energy system investments and operation. *Energy Conversion and Management 75*, 673–684.

Kerber, G. and R. Witzmann (2008). Statistische Analyse von NS-Verteilnetzen und Modellierung von Referenznetzen. *EW - Magazin für die Energiewirtschaft 107*(6), 22–26.

Lauster, M., J. Teichmann, M. Fuchs, R. Streblow, and D. Mueller (2014). Low order thermal network models for dynamic simulations of buildings on city district scale. *Building and Environment 73*, 223–231.

Lehnhoff, S., O. Nannen, S. Rohjans, F. Schlogl, S. Dalhues, L. Robitzky, U. Hager, and C. Rehtanz (2015). Exchangeability of power flow simulators in smart grid co-simulations with mosaik. In *2015 Workshop on Modeling and Simulation of Cyber-Physical Energy Systems (MSCPES)*, pp. 6 pp.

Mancarella, P. (2013). MES (multi-energy systems): An overview of concepts and evaluation models. *Energy*.

Mets, K., J. A. Ojea, and C. Develder (2014). Combining Power and Communication Network Simulation for Cost-Effective Smart Grid Analysis. *IEEE Communications Survey and Tutorials 16*(3), 1771–1796.

Molitor, C., S. Gross, J. Zeitz, and A. Monti (2014). MESCOS - A Multienergy System Cosimulator for City District Energy Systems. *IEEE Transactions on Industrial Informatics 10*(4), 2247–2256.

Molitor, C., M. Marin, L. Hernández, and A. Monti (2013). Decentralized coordination of the cooperation of residential heating units. In *Innovative smart grid technologies Europe*. Piscataway: IEEE.

Müller, D., M. Lauster, A. Constantin, M. Fuchs, and P. Remmen (2016). AixLib - An Open-Source Modelica Library within the IEA-EBC Annex 60 Framework. In J. Grunewald (Ed.), *Proceedings of the CESBP Central European Symposium on Building Physics and BauSIM 2016*, pp. 3–9. Stuttgart: Fraunhofer IRB Verlag.

Müller, D., A. Monti, S. Stinner, T. Schlösser, T. Schütz, P. Matthes, H. Wolisz, C. Molitor, H. Harb, and R. Streblow (2015). Demand side management for city districts. *Building and Environment 91*, 283–293.

Patteeuw, D., K. Bruninx, A. Arteconi, E. Delarue, W. D'haeseleer, and L. Helsen (2015). Integrated modeling of active demand response with electric heating systems coupled to thermal energy storage systems. *Applied Energy 151*, 306–319.

Remmen, P., M. Lauster, M. Mans, T. Osterhage, and D. Müller (2016). CityGML Import and Export for Dynamic Building Performance Simulation in Modelica. In *Proceedings of the 3rd IBPSA-England Conference BSO 2016, Great North Museum, Newcastle, 12th-14th September 2016.*

Richardson, I., M. Thomson, and D. Infield (2008). A high-resolution domestic building occupancy model for energy demand simulations. *Energy and Buildings 40*(8), 1560–1566.

Richardson, I., M. Thomson, D. Infield, and C. Clifford (2010). Domestic electricity use: A high-resolution energy demand model. *Energy and Buildings 42*(10), 1878–1887.

Rohjans, S., E. Widl, W. Müller, S. Schütte, and S. Lehnhoff (2014). Gekoppelte Simulation komplexer Energiesysteme mittels MOSAIK und FMI. *at - Automatisierungstechnik 62*(5).

Schloegl, F., S. Rohjans, S. Lehnhoff, J. Velasquez, C. Steinbrink, and P. Palensky (2015). Towards a classification scheme for co-simulation approaches in energy systems. In *2015 International Symposium on Smart Electric Distribution Systems and Technologies (EDST)*, Piscataway, NJ, pp. 516–521. IEEE.

Stinner, S., K. Huchtemann, and D. Müller (2016). Quantifying the operational flexibility of building energy systems with thermal energy storages. *Applied Energy 181*, 140–154.

Stinner, S., M. Schumacher, K. Finkbeiner, R. Streblow, and D. Müller (2015). FastHVAC - A library for fast composition and simulation of building energy systems. In *The 11th International Modelica Conference*, Linköping electronic conference proceedings, pp. 921–927. Linköping University Electronic Press.